International Journal of Cosmetic Science, 2003, **25**, 235–243

Two-stage kinetic analysis of fragrance evaporation and absorption from skin

P. Saiyasombati and G. B. Kasting
College of Pharmacy, The University of Cincinnati Medical Center, Cincinnati, OH 45267-0004, U.S.A.

Received 16 July 2003, Accepted 15 September 2003

Keywords: absorption, evaporation, fragrance, mathematical model, mixtures, skin

Synopsis

Human *in vivo* fragrance evaporation data from a previously published study are reanalysed in terms of compartmental pharmacokinetic models in which the microscopic rate constants are functions of the physicochemical properties of the fragrance components. According to the proposed analysis, which is restricted to low doses, absorption and evaporation of each component are first-order processes occurring from either the skin (one-compartment model) or the skin and a more rapidly depleted vehicle layer (two-compartment models). Evaporation rates of ingredients from a 12-component mixture containing a musk fixative followed single exponential decays that were well described by the one-compartment model. An otherwise identical mixture without fixative yielded evaporation rates that could be characterized as biexponential decays associated with loss from two compartments. This result shows that ingredient interactions qualitatively and quantitatively change evaporation rate profiles of fragrance components; however, an attempt to account for these interactions explicitly by means of activity coefficients inserted as multipliers for the microscopic rate constants was unsuccessful. Re-examination of this approach in the context of a diffusion/evaporation model is suggested. The developed models have potential utility for dermal risk assessment and for prediction of aroma evolution following topical application of complex fragrances.

Correspondence: Gerald B. Kasting, The University of Cincinnati Medical Center, PO Box 670004, Cincinnati, OH 45267-0004, U.S.A. Tel: +1 513 558 1817; fax: +1 513 558 0978; e-mail: Gerald.Kasting@uc.edu

Résumé

Des données d'une étude publiée précédemment sur l'évaporation de parfum de humaine *in vivo* sont réanalysées en utilisant des modèles pharmacocinétiques compartimentés dont les constants microscopiques de taux sont des functions des propriétés physio-chimiques des composants de parfum. Selon l'analyse proposée, qui est limitée aux petites doses, l'absorption et l'évaporation de chaque composant sont des processus de premier ordre se produisant l'un de la peau (modèle d'un compartiment), ou l'autre de la peau et d'une couche de véhicule plus rapidement épuisée (modèles de deux compartiments). Les taux d'évaporation d'ingrédients d'un mélange de 12 composants contenant un fixatif de musc suivi par des décompositions exponentielles uniques qui ont été bien décrites par le modèle d'un compartiment. Un mélange sans fixatif mais identique pour le reste a rapporté des taux d'évaporation qui pourraient être caractérisés commes des décompositions bi-exponentielles avec une perte de deux compartiments. Ce résultat montre que les interactions d'ingrédient changent qualitativement et quantitativement les profils de taux d'évaporation des composants de parfum. Cependant, une tentative d'expliquer précisement ces interactions au moyen des coefficients d'activité insérés comme multiplicateurs pour les constants microscopiques de taux n'a pas été réussie. Le réexamen de cette approche dans le contexte d'un modèle de diffusion/evaporation est suggéré. Les modèles développés ont une utilité potentielle dans l'évaluation des risques cutané et pour la prévision de l'évolution d'arome suivant l'application topique des parfums complexes.

Introduction

Fragrances are comprised of a complex mixture of ingredients designed to produce a pleasant and/or stimulating aroma following application to the skin. The aroma evolves over time, gradually decreasing in intensity as first the high notes (most volatile compounds) and then the middle and low notes (e.g. musks or other fixatives) dissipate through a combination of evaporation and absorption into the skin. A technical understanding of the dissipation process is important for two reasons: (i) it can aid in the design and evaluation of fine fragrances and other fragranced products [1]; and (ii) it can aid in the risk assessment process for these products with respect to both skin sensitization and systemic exposure [2]. We have previously described a one-compartment, first-order kinetic approach to modeling the disposition of fragrances on skin (Fig. 1a, Method 1) [3]. The method was used to correlate the evaporated fractions of each component of a 12-component fragrance mixture from human volar forearm [4] with physicochemical properties. More recently, we have extended this approach by explicitly considering the dry-down process immediately following application to the skin [5]. This was accomplished by adding a second compartment to the kinetic model to represent the solution or formulation applied to the skin surface. Two variations were considered (Fig. 1b, Method 2; Fig. 1c, Method 3). The modified models were able to better represent the kinetics of the evaporation and absorption processes for a model fragrance ingredient applied to human skin *in vitro* [5]. In this report, we show that the two-compartment models also improve the kinetic description of evaporation rates measured on human skin *in vivo*, using the previously analysed study of Vuilleumier *et al.* [4] as an example. Thus, they may be more useful than the one-compartment model as tools with which to correlate, and eventually predict, the changing composition of aromas arising from skin following topical application of a fine fragrance or a fragranced consumer product.

Theory

The compartmental models considered herein have been previously described [3, 5]. A brief synopsis is given below.

Model 1

The skin is assumed to be a single, well-stirred compartment that rapidly incorporates a topically applied ingredient (Fig. 1a). The amount of an ingredient that has evaporated at time t following application of amount A_0 at time zero is

$$A_{\text{air}}(t) = A_0\left(\frac{k_1}{k_1 + k_2}\right)\left[1 - \mathrm{e}^{-(k_1+k_2)t}\right] \qquad (1)$$

where k_1 is the evaporation rate constant and k_2 is the absorption rate constant. The rate constants for each compound are functions of temperature T, surface airflow v, and three physico-chemical properties: vapour pressure P_{vp}, molecular weight MW, and lipid solubility S_{oct}. The latter is taken to be solubility in *n*-octanol, expressed as the product of water solubility S_{w} and octanol–water partition-coefficient K_{oct}. Each property is expressed in dimensionless, or 'reduced', form by dividing by a characteristic value; thus,

$$k_1 = k_1^v \cdot P_{\text{vpr}} / (K_{\text{oct}} \cdot S_{\text{w}})_r \qquad (2)$$

$$k_2 = k_2^T \cdot \text{MW}_r^{-2.7} \qquad (3)$$

In Equations 2 and 3, $P_{\text{vpr}} = P_{\text{vp}}/1$ torr, $(K_{\text{oct}} \cdot S_{\text{w}})_r = (K_{\text{oct}} \cdot S_{\text{w}})/1000$ g cm^{-3} and $\text{MW}_r = \text{MW}/100$ Da. The constants k_1^v and k_2^T are dependent on surface airflow and temperature, respectively. They have the same value for all fragrance components. The fraction evaporated after a long time ($t \to \infty$) is

$$f_{\text{evap}} = \frac{k_1}{k_1 + k_2} = \frac{x_r}{k + x_r} \qquad (4)$$

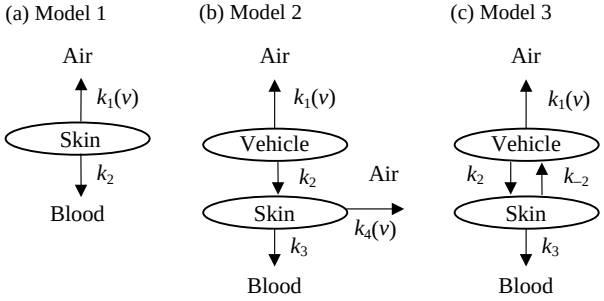

Figure 1 Schematic diagrams for compartmental models of skin disposition. (a) One compartment (Model 1); (b) two compartments with evaporation from vehicle and skin (Model 2); and (c) two compartments with evaporation from vehicle only (Model 3).

where $k = k_2^T/k_1^v$ and $x_r = P_{vpr}MW_r^b/(K_{oct} \cdot Sw)_r$. The variation of k_1^v and k_2^T with airflow and temperature are discussed in [5] and [3], respectively. In this report, these conditions do not vary; thus, k_1^v and k_2^T are treated as constants to be determined from the data.

Model 2

In this model, there are two well-stirred compartments – one representing the surface film (or vehicle), the other representing the skin (e.g. the stratum corneum) (Fig. 1b). All ingredients are initially present in the vehicle only. Evaporation is assumed to occur first from the vehicle, which is rapidly depleted by the combination of this process with partitioning into the skin. Subsequent evaporation and absorption occur from the skin compartment. The amount of an ingredient that has evaporated at time t following application of amount A_0 at time zero is

$$A_{air}(t) = \frac{A_0}{\alpha\beta(\beta-\alpha)}\left\{[k_1(\beta-\alpha)+k_2k_4]\beta\left(1-e^{-\alpha t}\right)\right.$$
$$\left.-k_2k_4\alpha\left(1-e^{-\beta t}\right)\right\} \quad (5)$$

where $\alpha = k_1 + k_2$ and $\beta = k_3 + k_4$. After a long time, the fraction evaporated is

$$f_{evap} = \frac{1}{\alpha\beta}(k_1k_4 + k_1k_3 + k_2k_4)$$
$$= \frac{k_1k_4 + k_1k_3 + k_2k_4}{k_1k_4 + k_1k_3 + k_2k_4 + k_2k_3} \quad (6)$$

The evaporation rate constants k_1 and k_4 are considered to have the physical properties dependency shown in Equation 2. This is a Henry's Law-like relationship in which evaporative loss from a surface is assumed to be proportional to equilibrium vapour pressure, P_{vp}, and inversely proportional to solubility in the matrix. Both vehicle and skin are considered to be lipidic matrices with properties similar to *n*-octanol. The vehicle-to-skin rate constant k_2 and the absorption rate constant k_3 are assigned the molecular weight dependence described by Equation 3. This relationship follows from steady-state skin permeability properties in the limit of small applied doses [3]. The rationale for both these physical properties dependencies is presented in [3]. Under these assumptions, Equation 6 can be rewritten in terms of the reduced physical properties ratio x_r defined in Equation 4. The result may be expressed as

$$f_{evap} = \frac{x_r}{k' + x_r} \quad (7)$$

where

$$k' = \frac{k_2^Tk_3^T}{k_1^vk_3^T + k_2^Tk_4^v + k_1^vk_4^vx_r} \quad (8)$$

Equations 7 and 8 are written as shown to emphasize the analogy with Equation 4, although in this case the factor k' is not a constant (thus, Equation 7 represents a modified hyperbola).

Model 3

This model is similar to Model 2, except that the vehicle layer persists much longer, remaining as a discrete film until the last of the components has completely dissipated (Fig. 1c). A situation corresponding to either of these models might occur in practice, with the more volatile and/or skin-permeable films dissipating according to Model 2 and less volatile/permeable films dissipating according to Model 3. The amount of an ingredient that has evaporated at time t following application of amount A_0 at time zero is

$$A_{air}(t) = \frac{k_1A_0}{\alpha\beta(\beta-\alpha)}\left[(k_{-2}+k_3-\alpha)\beta\left(1-e^{-\alpha t}\right)\right.$$
$$\left.+(\beta-k_{-2}-k_3)\alpha\left(1-e^{-\beta t}\right)\right] \quad (9)$$

where $-\alpha$ and $-\beta$ are the roots of the equation $x^2 + (\alpha+\beta)x + \alpha\beta = 0, \alpha+\beta = k_1 + k_2 + k_{-2} + k_3$ and $\alpha\beta = k_1k_{-2} + k_1k_3 + k_2k_3$. After a long time, the fraction evaporated is

$$f_{evap} = \frac{k_1}{\alpha\beta}(k_{-2} + k_3) \quad (10)$$

In Model 3, the evaporation rate constant k_1 is assumed to have the physical properties dependency shown in Equation 2, and the remaining rate constants are assumed to vary with molecular weight as in Equation 3. Such an assignment is consistent with the dependencies assumed for Models 1 and 2. With these choices, Equation 10 may be rewritten as:

$$f_{evap} = \frac{x_r}{k'' + x_r} \quad (11)$$

where

$$k'' = \frac{k_2^Tk_3^T}{k_1^v\left(k_{-2}^T + k_3^T\right)} \quad (12)$$

Thus, Model 3 leads to a hyperbolic relationship between evaporated fraction and x_r, similar to Model 1.

Methods

Overview

The Vuilleumier *et al.*'s study involved trapping and GC analysis of volatiles arising from the skin following topical application of two closely related fragrance compositions to the forearm of a single human volunteer [4]. Trapped volatiles were analysed at eight time points spaced between 0.25 and 7.25 h. The compositions and the physical properties of the ingredients are listed in Table I. Vector A comprised the first 11 of these ingredients. Vector B differed from Vector A in that a musk or fixative agent (Compound XII) was included in the composition. Addition of the musk led to a reduction in the initial evaporation rates of the other components, as noted by the original workers (cf. also [3]). The present analysis focuses on the different kinetic profiles displayed by the two fragrance vectors.

Cumulative evaporation data for each ingredient, normalized by applied dose, were calculated as described previously [3]. Average evaporation rates over each time interval were calculated and plotted semilogarithmically versus time. The rate constants for kinetic models 1–3 were fit to the data for each ingredient by non-linear least squares using the two different weighting schemes described below. The physical properties were then deconvolved from the rate constants using Equations 2 and 3 (and equivalent expressions for the other rate constants – see Theory section) to give the compound-independent proportionality constants k_1^v, k_2^T, k_3^T, etc. The latter values were averaged across compounds in a sequential manner (see below) to give the values reported. Finally, the average values were used to simulate the evaporation profiles for all of the compounds. Thus, in the final step of the analysis, the evaporation rates for 11 compounds (Vector A) or 12 compounds (Vector B) were calculated based on three physico-chemical properties (P_{vp}, S_{oct} and MW) and either two (Model 1) or four (Models 2 and 3) adjustable parameters.

In conducting this analysis, Compounds XI and XII were excluded from the fitting procedure, as the extent of evaporation was not sufficient to allow an unambiguous determination of the rate constants (cf. [3]). However, they were included in the simulation phase of the analysis. Comparison of the calculated and observed evaporation profiles for these compounds is an unbiased, albeit limited, test of the predictive power of the derived models.

Table I Fragrance raw materials analysed in this report (data from [3] and [4])

ID	Compound	MW, Da	P_{vp}[a], torr	Log K_{oct}[a]	S_w[a], g L^{-1}	x_r, Equation 4	f_{evap}[b] Vector A	f_{evap}[b] Vector B
I	Linalool	154	0.13	2.55	2.3	0.52	0.681 ± 0.004	0.575 ± 0.015
II	Dihydromyrcenol	156	0.19	3.03	0.76	0.79	0.735 ± 0.016	0.658 ± 0.022
III	10-Undecanal	170	0.093	4.05	0.072	0.48	0.594 ± 0.004	0.452 ± 0.061
IV	Citronellol	156	0.028	3.25	0.46	0.11	0.500 ± 0.004	0.412 ± 0.007
V	2-Phenyl-1-ethanol	122	0.039	1.36	35	0.08	0.260 ± 0.003	0.186 ± 0.020
VI	(E)-cinnamic alcohol	134	0.0050	1.95	8.5	0.01	0.039 ± 0.004	0.037 ± 0.006
VII	Alpha-damascone	192	0.032	3.62	0.19[c]	0.28	0.712 ± 0.007	0.570 ± 0.028
VIII	*Cis*-7-*p*-menthanol	156	0.019	3.33	0.38	0.08	0.545 ± 0.014	0.469 ± 0.054
IX	2,2,2-Trichloro-1-phenyl-ethylacetate	268	0.0029	4.05	0.072[c]	0.08	0.422 ± 0.004	0.405 ± 0.032
X	M.P.C.C.[d]	192	0.010	3.87	0.11	0.07	0.330 ± 0.005	0.237 ± 0.022
XI	(E)-2-benzylideneoctanal	216	0.00088	4.85	0.011[c]	0.01	0.069 ± 0.007[e]	0.043 ± 0.007[e]
XII	15-Pentadecanolide	240	0.00010	5.35	0.0034[c]	0.001	NA[f]	0.066 ± 0.010[e]

[a]For sources of physical properties, see [3].
[b]Experimental fraction of dose evaporated, extrapolated to $t \to \infty$ (except for XI and XII) [3].
[c]Estimated value, corrected from [3].
[d]3-(4-methyl-3-pentenyl)-3-cyclohexene-1-carbaldehyde + 4-(4-methyl-3-pentenyl)-3-cyclohexene-1-carbaldehyde.
[e]0–7.25 h only.
[f]This ingredient (a musk fixative) was included in Vector B, but not in Vector A.

Least squares fitting procedure

The parameters in each model were sequentially optimized by the method described previously [5]. The order of optimization was k_2^T followed by simultaneous determination of the other parameters. The sum of squared residuals $SSR = \sum_i w_i\ [y_i(\text{obs}) - y_i(\text{fit})]^2$ (or, equivalently, the reduced chi-square value, $\chi_v^2 = SSR/(n-p)$, where n is the number of observations and p is the number of adjustable parameters [6]) was minimized for two different choices of the dependent variable y_i and the corresponding weights w_i. In the first (cumulative) version, y_i was taken to be the cumulative amount of each ingredient evaporated at time t_i, and $w_i = 1$. This is the fitting procedure used in [5]. In the second (incremental) version, y_i was taken to be the incremental amount evaporated between times t_{i-1} and t_i, and $w_i = 1/y_i^2$. This procedure minimized the relative errors in Δ(amount evaporated) at each time point; thus, it was much more sensitive to low evaporation rates occurring at later times in the study. For Models 2 and 3, the two weighting schemes gave substantially different parameter values.

Results

Representative semilogarithmic plots of evaporation rates versus time are shown in Figs. 2 and 3. After the first 15 min, most of the data plotted in this manner were either linear or reasonably so; this was the basis of the one-compartment kinetic analysis presented in [3]. However, closer examination of these data revealed a systematic difference between Vector A (11-component mixture without fixative) and Vector B (12-component mixture with fixative). For most ingredients, the presence of the fixative agent – a musk, Compound XII – depressed the initial evaporation rate and increased the rate after 4–6 h. This led to log linear evaporation rate profiles for these components in Vector B (e.g. Fig. 2b) and curvilinear profiles for the same components in Vector A (e.g. Fig. 2a). This effect was especially pronounced for compounds having high volatility – the so-called 'top notes' like linalool and limonene. Several of the plots also revealed a low evaporation rate for the initial 0–15-min interval. This effect may be attributed to a lag time for vapor collection resulting from the finite headspace between the skin surface and the vapor trap, as discussed elsewhere [5].

Optimized parameters resulting from the kinetic model data analysis are shown in Table II. Model 1 (one-compartment) was found to adequately represent both the cumulative evaporation and the evaporation rate profiles for the components of Vector B. Examples of such fitted curves are shown in Fig. 2(d,b), respectively. This finding is consistent with our earlier analysis of these data [3] and with

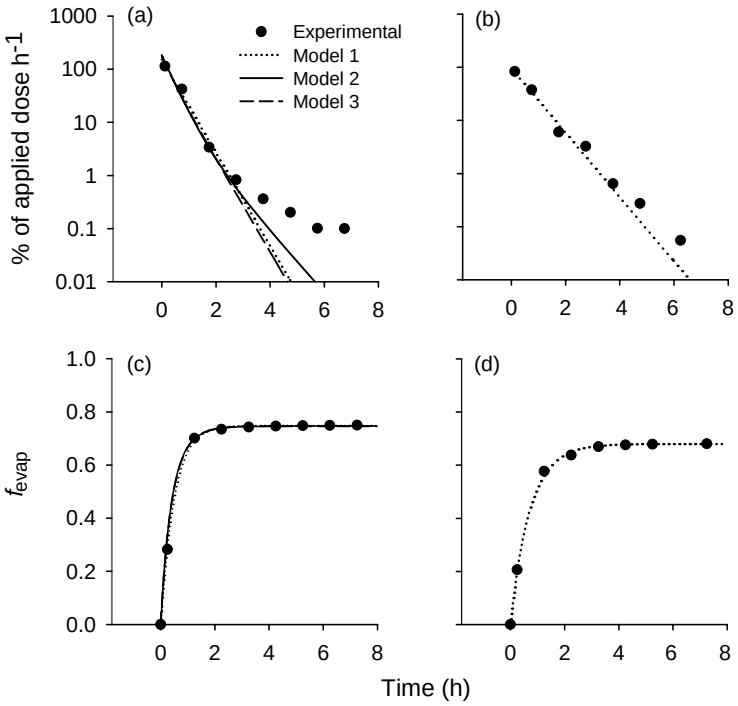

Figure 2 Evaporation of dihydromyrcenol (Compound II, Trial 2) from human skin *in vivo* [4]. (a) Evaporation rate, Vector A; (b) evaporation rate, Vector B; (c) cumulative evaporation, Vector A; and (d) cumulative evaporation, Vector B. The model calculations were based on the cumulative fitting procedure.

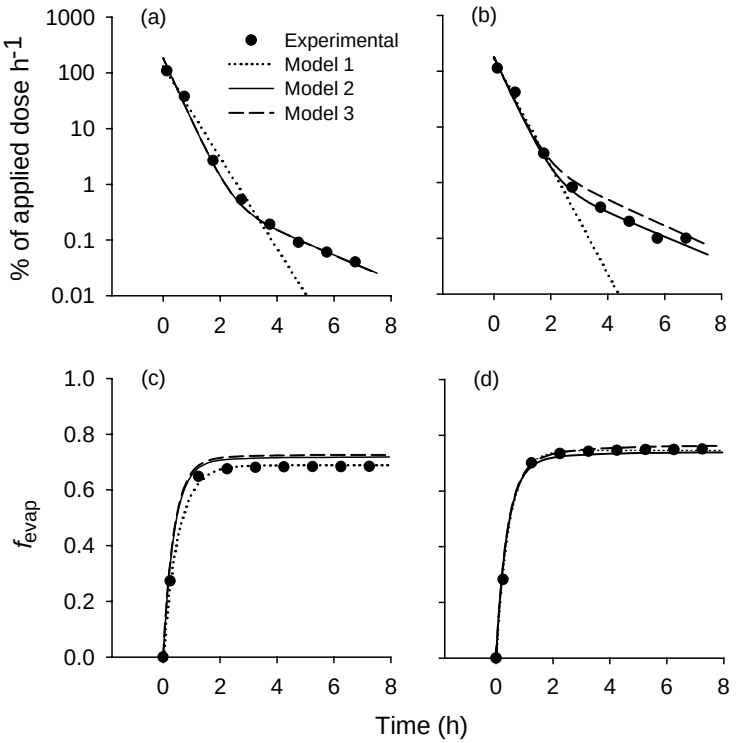

Figure 3 Evaporation of linalool (Compound I) and dihydromyrcenol (Compound II) from human skin *in vivo*, following application in Vector A, Trial 2 [4]. (a) Evaporation rate, Compound I; (b) evaporation rate, Compound II; (c) cumulative evaporation, Compound I; and (d) cumulative evaporation, Compound II. The model calculations were based on the incremental fitting procedure.

the single exponential decay of the evaporation rates in this vector. Models 2 and 3 (two-compartments) offered no improvement in the fit; in fact, it was not possible to obtain unambiguous parameter values for these models when applied to the Vector B data.

The findings for Vector A were substantially different. Model 1 still provided an adequate description of the cumulative evaporation versus time curves (cf. Figs. 2c,d and 3c,d). However, the evaporation and absorption rate constant prefactors, k_1^v and k_2^T, obtained for Vector A (Table II, Model 1) were significantly larger than those for Vector B ($P = 0.044$ and 0.014, respectively, by one-tailed Student's *t*-test). Furthermore, it was not possible to describe the details of the evaporation rate profiles for Vector A (cf. Figs. 2a and 3a,b) using Model 1. The

Table II Regression parameters (mean ± SD, 20 determinations per vector) for compartmental models of fragrance evaporation

		Model 1			
Parameter	**Units**	**Vector A**	**Vector B**	**Model 2 Vector A**	**Model 3 Vector A**
k_1^v	h^{-1}	14.5 ± 10.5	9.1 ± 8.9	14.1 ± 9.5	14.3 ± 9.8
k_2^T	h^{-1}	1.9 ± 0.6	1.5 ± 0.5	2.5 ± 0.7	2.4 ± 0.7
k_{-2}^T	h^{-1}	–	–	–	0.9 ± 1.7
k_3^T	h^{-1}	–	–	1.3 ± 1.1	1.9 ± 1.8
k_4^v	h^{-1}	–	–	1.9 ± 2.5	–
Regression statistics (cumulative fits)					
n		143	132	143	143
s		0.13	0.16	0.15	0.14
r^2		0.7960	0.7333	0.7835	0.7903
χ_ν^2		0.017	0.026	0.021	0.018

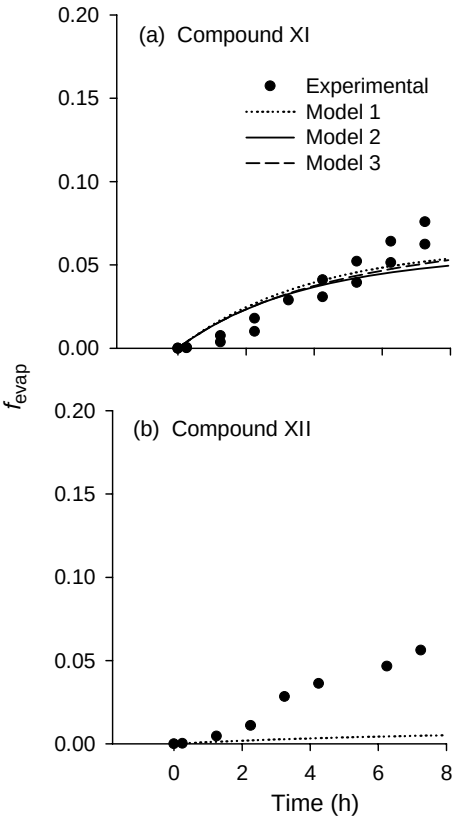

Figure 4 Cumulative evaporation of (E)-2-benzylideneoctanal (Compound XI) and 15-pentadecanolide (Compound XII) from human skin *in vivo* [4]. (a) Compound XI, Vector A and (b) Compound XII, Vector B. The model calculations were based on the average parameters reported in Table II.

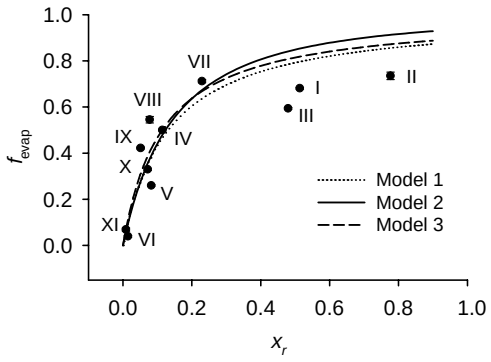

Figure 5 Predicted and observed values of the total evaporated fractions of each component in Vector A (mean ± SD of Trials 1 and 2) plotted versus the physical properties ratio x_r (Equation 4). The error bars are smaller than the symbols. The model curves were calculated from Equations 4, 7 and 11 using the parameters in Table II.

evaporation rates for most Vector A components simply could not be described as a single exponential decay.

The two-compartment models, Models 2 and 3, yielded better descriptions of the Vector A evaporation rates. However, in order to obtain a suitable match to the 'tail' of these plots, i.e. the evaporation rates at times longer than 4 h, it was necessary to use the incremental model fitting procedure described in the Methods section. This may be seen by comparing the theoretical curves in Fig. 2(a) (cumulative fits) with those in Fig. 3(a,b) (incremental fits). The incremental procedure minimized differences in the small amounts evaporated at longer times, with a concurrent sacrifice in describing the cumulative evaporation profiles. However, the loss in the latter area was small (cf. Figs. 2c,d and 3c,d) and would not seem to preclude the use of Models 2 and 3 in exposure assessment (cf. Figs. 2c and 3c). Qualitatively, Model 2 led to slightly better descriptions of evaporation rates than did Model 3 (e.g. Fig. 3b), in agreement with a previous report [5]. However, there was no significant difference between the χ^2_ν values for Models 2 and 3 (Table II).

By employing the optimized parameters from the analysis of Compounds I–X, we found that all three models could also satisfactorily predict the total evaporated fractions of Compound XI in both Vector A (Fig. 4a) and Vector B. However, the evaporation of the musk (Compound XII) was found to be highly underpredicted (Fig. 4b). Another compound whose evaporation rate was poorly predicted was cinnamic alcohol (Compound VI). Using the parameters in Table II, the calculated evaporation rate for cinnamic alcohol according to Models 1–3 was three times greater than the observed rate. It is not known whether the discrepancies observed for Compounds VI and XII reflect ingredient interactions, inaccurate estimates of the vapor pressures, or chemical reactivity on the skin. These differences warrant further investigation.

Figure 5 shows the cumulative fraction evaporated for each compound in Vector A (extrapolated to $t \rightarrow \infty$ as in [3]) plotted vs. the physical properties ratio x_r defined in Equation 4. Larger values of x_r lead to higher evaporated fractions and, by inference, lower absorbed fractions, of the various fragrance components. Models 1–3 captured a substantial part of this behaviour; however, the evaporation of the most volatile compounds was overestimated by each approach. No significant difference was found in the ability of Models 1–3 to describe these data ($P > 0.6$ based on a two-way ANOVA).

Discussion

The present analysis shows a systematic difference between the evaporation profiles of two nearly identical fragrance mixtures, which differed only in the presence (Vector B) or absence (Vector A) of the musk fixative, Compound XII. It is generally recognized that a fragrance fixative retards the evaporation of fragrance components in order to increase the life of a perfume on skin. Quantitative analysis (e.g. Fig. 2a,b) supports this notion, as evaporation rates of dihydromyrcenol are sustained longer in Vector B than in Vector A. These findings and chemical intuition suggest that the musk lowers the thermodynamic activity of the other fragrance ingredients, thereby retarding both absorption and evaporation. The effect appears to be greatest for the most volatile components.

The kinetic models described here provide a way of quantifying the differences in evaporation rates between fixed and unfixed fragrances. We found a one-compartment model (Model 1) to be adequate for the fixed fragrance, Vector B, whereas two-compartment models (Models 2 or 3) provided a better fit to the data for Vector A. However, none of these models account explicitly for the ingredient interactions leading to the observed differences between Vectors A and B. In order to do so, it would seem appropriate to extend the analysis to a true diffusion/evaporation model incorporating activity coefficients to represent the interactions. Using the present data set, we experimented with this idea by applying activity coefficients calculated by the UNIFAC/UNIQUAC approach [7] as multipliers to the kinetic rate coefficients, as described elsewhere [5]. Consistent with the previous finding, this approach failed to yield an improved description of the results. A longer term goal of our work is to develop a plausible and computationally manageable way of accounting for such ingredient interactions. This would seem to be critical in order to make accurate predictions for complex fragrance mixtures containing fixatives and for fragranced personal care products containing many other ingredients.

Both the one-compartment (Model 1) and two-compartment (Models 2 and 3) kinetic models yielded reasonable correlations with total evaporated fraction of each component (cf. Fig. 5). The largest relative errors in calculated evaporation rates were for the musk (Compound XII, 10-fold underestimation) and cinnamic alcohol (Compound VI, threefold overestimation). In the absence of significant chemical reactivity or binding to skin, this correlation implies a corresponding relationship between physical properties and fraction of dose absorbed, as $f_{abs} = 1 - f_{evap}$ in this case. Using this approach to estimate absorption, it is evident from Fig. 5 that the largest relative errors would occur for the highly volatile components, Compounds I–III, where underestimates of two- to threefold might be anticipated. It is possible to improve the agreement of the models with the cumulative evaporation (and estimated total absorption) data by fitting only the cumulative results, e.g. by adjusting the parameters k, k' and k'' in Equations 4, 7, and 11. Such a procedure, which was employed in [3] to estimate k, may have value for systemic absorption estimation in dermal risk assessment. However, it would most likely lead to poorer representations of the evaporation rate profiles. Thus, for investigators interested in quantifying the duration of aromas on skin, it would seem the two-compartment models with parameter values similar to those in Table II may have more utility than the one-compartment or cumulative data fitting approaches.

Conclusions

A kinetic analysis of previously reported fragrance evaporation data on skin has shown both qualitative and quantitative differences between evaporation profiles from fixed and unfixed fragrances. The fixed fragrance (Vector B) led to nearly first-order evaporation kinetics that were well described by a one-compartment model. The unfixed fragrance (Vector A) led to more complex kinetics that could be approximated by a biexponential decay. Two alternative two-compartment models were developed to simulate this behaviour. The analysis provides strong evidence for interactions of the more volatile fragrance components with fixative agents that may be explainable on a thermodynamic basis.

Acknowledgements

P.S. thanks the University of Cincinnati for a Distinguished Dissertation fellowship. The work was supported by the Procter & Gamble Company's International Program for Animal Alternatives, the University of Cincinnati, and NIOSH grant R01 OH007529-01.

References

1. Mookherjee, B.D., Patel, S.M., Trenkle, R.W. and Wilson, R.A. A novel technology to study the emission of fragrance from the skin. *Perfumer Flavorist* **23**, 1–11 (1998).

2. Gerberick, G.F. and Robinson, M.K. A skin sensitization risk assessment approach for evaluation of new ingredients and products. *Am. J. Contact Derm.* **11**, 65–73 (2000).
3. Kasting, G.B. and Saiyasombati, P. A physico-chemical properties based model for estimating evaporation and absorption rates of perfumes from skin. *Int. J. Cosmet. Sci.* **23**, 49–58 (2001).
4. Vuilleumier, C., Flament, I. and Sauvegrain, P. Headspace analysis study of evaporation rate of perfume ingredients applied onto skin. *Int. J. Cosmet. Sci.* **17**, 61–76 (1995).
5. Saiyasombati, P. and Kasting, G.B. Disposition of benzyl alcohol following topical application to human skin *in vitro*. *J. Pharm. Sci.* **92**, 2128–2139 (2003).
6. Bevington, P.R. *Data Reduction and Error Analysis for the Physical Sciences*. McGraw-Hill, New York (1969).
7. Reid, R.C., Prausnitz, J.M. and Poling, B.E. *The Properties of Liquids and Gases*. McGraw-Hill, New York (1987).